

RESEARCH

Open Access



PTOV1 exerts pro-oncogenic role in colorectal cancer by modulating SQSTM1-mediated autophagic degradation of p53

Yongli Fan^{1†}, Yuqin Li^{2†}, Xia Luo^{3†}, Shiqi Xiang⁴, Jia Hu⁴, Jingchun Zhan⁸, Weilong Chang⁶, Rui Deng⁶, Xianwen Ran⁷, Yize Zhang⁵, Yudie Cai⁵, Weiwei Zhu⁵, Huifen Wang^{5*}, Zhibo Liu^{6,7*}  and Di Wang^{6*} 

Abstract

Background Prostate Tumor Overexpressed 1 (PTOV1) is overexpressed and associated with malignant phenotypes in various types of tumors. However, the detailed roles of PTOV1 and its underlying mechanism in CRC remain unclear.

Methods The clinical significance of PTOV1 was assessed in clinical databases and CRC samples. The effects of PTOV1 on the tumor-associated phenotypes of CRC were detected by several in vitro assays and in vivo mouse models. Immunoprecipitation (IP) combined with protein mass spectrometry and Co-Immunoprecipitation (Co-IP) was used to identify p53 interacting with PTOV1. Immunofluorescence assay, western blot and transmission electron microscopy (TEM) analysis were used to evaluate the effects of PTOV1 on autophagy.

Results Here, we revealed that PTOV1 was highly expressed in human CRC tissues, especially at advanced stages, and associated with reduced survival time among CRC patients. The upregulated PTOV1 promoted cell proliferation, migration, invasion, tumor growth and metastasis of CRC cells in vitro and in vivo. At the molecular level, PTOV1 destabilized p53 by activating autophagy and recruiting p53 for the cargo receptor SQSTM1 directed autophagic degradation. There was a negative expression correlation between PTOV1 and p53 in CRC tissues. Moreover, p53 overexpression or SQSTM1 knockdown reversed the pro-tumor phenotypes of PTOV1 in CRC.

Conclusion Our study unveils the oncogenic role of PTOV1 in CRC progression, which was achieved by promoting SQSTM1 directed autophagic degradation of p53. These findings highlight the potential of targeting the PTOV1-SQSTM1-p53 axis as a therapeutic approach for CRC.

Keywords Colorectal cancer, Autophagy, PTOV1, p53

[†]Yongli Fan, Yuqin Li and Xia Luo contributed equally to this work.

*Correspondence:

Huifen Wang
wanghf1011@163.com
Zhibo Liu
lz11041100271@163.com
Di Wang
diwangwhuh@126.com

Full list of author information is available at the end of the article



© The Author(s) 2025. **Open Access** This article is licensed under a Creative Commons Attribution-NonCommercial-NoDerivatives 4.0 International License, which permits any non-commercial use, sharing, distribution and reproduction in any medium or format, as long as you give appropriate credit to the original author(s) and the source, provide a link to the Creative Commons licence, and indicate if you modified the licensed material. You do not have permission under this licence to share adapted material derived from this article or parts of it. The images or other third party material in this article are included in the article's Creative Commons licence, unless indicated otherwise in a credit line to the material. If material is not included in the article's Creative Commons licence and your intended use is not permitted by statutory regulation or exceeds the permitted use, you will need to obtain permission directly from the copyright holder. To view a copy of this licence, visit <http://creativecommons.org/licenses/by-nc-nd/4.0/>.

Introduction

Colorectal cancer (CRC) is the second leading cause of cancer related deaths, and its incidence is increasing rapidly worldwide [1, 2]. It is of great significance to clarify the mechanisms underlying CRC tumorigenesis and progression, and develop novel therapeutic targets. Prostate Tumor Overexpressed 1 (PTOV1), first identified in a differential screening for gene expression in prostate cancer, is overexpressed and associated with malignant phenotypes in various types of tumors, such as epithelial ovarian cancer, breast cancer and liver cancer [3–6]. PTOV1 is proposed to be a potential therapeutic target for pan-cancer treatment. However, the detailed roles of PTOV1 and its underlying mechanism in CRC remain elusive.

The transcription factor p53, a critical tumor suppressor, is activated and induces efficient cell death in cancer cells upon various stresses [7, 8]. The expression and activity of p53 are under exquisitely fine regulation in normal cells [9]. However, the loss of function (p53 mutants) or abnormal degradation of p53 is a common event and is considered to be a crucial driver of tumorigenesis, especially in CRC [10, 11]. Ubiquitin-proteasome and autophagy-lysosome are two main pathways involved in controlling cellular protein stability [12]. p53 can be degraded through both proteasome and autophagy-lysosome pathways [13, 14]. The proteasome-dependent degradation of p53 is well established. A series of E3 ligases, such as MDM2 [15], COP1 [16], and TRIM21 [17], are reported to participate in the ubiquitination regulation of p53. However, little is known about the upstream molecules that mediate the degradation of p53 through autophagy.

Here, we found that PTOV1 was upregulated in CRC tumor tissues and associated with poor clinical outcomes of CRC patients. Functional studies demonstrated that PTOV1 facilitated tumor growth and metastasis in CRC. Mechanistically, overexpression of PTOV1 induced autophagy and recruited p53 for autophagic degradation, a process mediated by autophagy receptor SQSTM1. PTOV1 expression was negatively associated with p53 in CRC tissues. Moreover, PTOV1 promoted CRC progression in a SQSTM1-dependent manner. This work uncovered the functional roles and mechanisms of PTOV1 in promoting CRC progression, which might provide new targets for CRC treatment.

Methods

Antibodies and reagents

The primary antibodies and reagents used in this study were as showed in Table S1.

Cell lines and transfection

HEK293T cells and human colorectal cancer cell lines HCT116, RKO, LoVo and DLD-1 were purchased from

the American Type Culture Collection (ATCC). These cell lines were all cultured in Dulbecco's Modified Eagle Medium (DMEM, Gibco) supplemented with 10% fetal bovine serum (FBS, PAN Biotech) and maintained in a cell humidified incubator at 37 °C with 5% CO₂. Cells were transfected with plasmids using Lipofectamine 3000 (Invitrogen) according to the manufacturer's instructions. Briefly, plate cells could be 70–90% confluent at the time of transfection, prepare plasmid DNA & siRNA-lipid complexes and add DNA-lipid complexes to cells, cell was harvested and analyzed after transfection for 48 h.

Plasmids construction

Human PTOV1 was amplified from cDNA library of HCT116 cells and cloned into pLenti-CMV-puro, pcDNA3.1/Myc-His, pFLAG-CMV or HA-CMV vectors, respectively. PTOV1 truncations (pFLAG-CMV-PTOV1_{1–234} and pFLAG-CMV-PTOV1_{253–416}) were constructed on the basis of pFLAG-CMV-PTOV1 plasmid by using polymerase chain reaction (PCR) method. Human p53 cDNA was amplified from cDNA library of HEK293T cells and cloned into HA-CMV or pLenti-neo vectors. p53 truncations (HA-p53_{1–94}, HA-p53_{95–393}, HA-p53_{95–292}) were constructed based on HA-p53 plasmid. shRNAs targeting human SQSTM1, PTOV1 or non-specific control shRNA were designed and inserted into pLKO.1-puro or pLKO.1-neo lentiviral vectors. All plasmids used in this study were confirmed by DNA sequencing. The primer sequence for plasmids construction in this study were listed in Supplemental Table S2.

Lentiviral transduction

HEK293T cells were co-transfected with indicated lentiviral vector, psPAX2 and pMD2.G plasmids to produce lentiviral particles. The supernatant containing lentiviral particles was harvested at 48–72 h post transfection. CRC cells were infected with lentiviral particles and further selected by puromycin (Selleck, 1 µg/mL) or neomycin (Beyotime, 300 µg/mL) for 1 weeks. The knockdown and overexpression efficiency of PTOV1 was validated by western blot. The shRNA sequences used in this study were listed in Supplemental Table S3.

Western blot analysis

Total proteins were extracted by RIPA lysis buffer (Beyotime) supplemented with protease inhibitors (MCE), and phosphatase inhibitors (MCE). Then the cell lysates were scraped, lysed on ice for 30 min and centrifuged at 12,000 rpm for 10–15 min. The supernatants were collected and the protein concentration was determined by the BCA kit (Thermo Scientific). 30 µg amount of protein was added with protein loading buffer (ACE) and denatured at 100 °C for 10 min, then separated by 12%

SDS-PAGE (Epizyme) and transferred to nitrocellulose membranes (Pall). The nitrocellulose membranes were blocked with 5% skim milk (Epizyme) for 1 h at room temperature and incubated with indicated primary antibodies overnight at 4 °C. The dilution of antibodies were as follows: GAPDH (1:5000), GFP-tag (1:2000), C-MYC (1:1000), Flag-tag (1:2000), HA-tag (1:2000), p62/SQSTM1 (1:4000); LC3 (1:2000); ATG7 (1:1000), ULK1 (1:1000), E-cadherin (1:1000), N-cadherin (1:1000), CyclinD1 (1:1000), β -catenin (1:2000), PI3K (1:1000) AKT (1:1000), p- β -catenin (1:1000), p-PI3K (1:1000), p-AKT (1:1000), PTOV1 (1:1000), p53 (1:200). After incubating with appropriate HRP-coupled secondary antibodies (1:5000) for 1 h at room temperature, the signals were detected by the chemiluminescence system (Odyssey, USA).

Co-immunoprecipitation analysis

CRC cells transfected with indicated plasmids were collected and lysed with western & IP lysis buffer (Beyotime) containing protease inhibitor. The supernatant of cell lysates was incubated with 2 μ g indicated antibodies at 4 °C overnight. Subsequently, protein A/G agarose beads (Santa Cruz Biotechnology) were added to incubation for another 2 h. After being washed by washing buffer for three times, the beads were boiled at 98 °C for 10 min in protein loading buffer and then subjected to western blot analysis.

Liquid chromatograph-mass spectrometry (LC-MS) analysis

FLAG-PTOV1 stably overexpression CRC cells were collected and lysed with Western & IP lysis buffer containing protease inhibitor. The supernatant of cell lysates was incubated with 2 μ g anti-FLAG antibody at 4 °C overnight. Subsequently, protein A/G agarose beads were added to incubation for another 2 h. After being washed by washing buffer for three times, the immunoprecipitated proteins were eluted and then subjected to liquid chromatograph-mass spectrometry (LC-MS) analysis.

Immunofluorescence assay

For immunofluorescent staining, cells were fixed with 4% paraformaldehyde, permeabilized with 0.5% Triton X-100 for 10 min (Sigma), blocked with 10% FBS (PAN Biotech), followed by staining with the indicated primary antibodies (1:100) overnight at 4 °C and secondary antibodies (1:200) for 1 h at room temperature. Subsequently, Hoechst 33,342 (1:1000) was used to stain nuclei for 5 min at room temperature. The photographs were imaged with a laser-scanning confocal microscope (Zeiss, USA).

Transmission electron microscopy (TEM) analysis

HCT116 cells were fixed with 2.5% glutaraldehyde (pH 7.4) for 2 h at 4 °C and 1% OsO₄ (pH 7.2) at room temperature for another 1.5 h. Then cells were dehydrated in a graded series of ethanol, embedded into ultracut (Leica UC7) and sectioned to 60 nm. Ultrathin sections were stained with uranyl acetate and lead citrate, then observed with an electron microscope (FEI Tecnai G20, USA).

EdU-DNA synthesis assay

BeyoClick™ EdU-594 (Beyotime) & BeyoClick™ EdU-488 (Beyotime) was used to assess the proliferation ability of CRC cells. The EdU solution was added for 2 h. After removal of the medium, the cells were fixed and permeated by 0.3% Triton X-100. Subsequently, the cells were incubated with Click reaction solution at room temperature for 30 min. Hoechst 33,342 (1:1000) was used to stain nuclei. The photographs were imaged with a laser-scanning confocal microscope (Olympus).

Transwell assay

For migration and invasion transwell assay, 1.0×10^4 CRC cells was resuspended in 200 μ l DMEM without serum and seeded in the upper chambers (Corning Inc.,3342) without or with matrigel matrix (BD Science). The lower chamber was added with 500 μ l DMEM supplied with 10% FBS. After maintained in a cell humidified incubator for appropriate duration, cells were fixed and stained with 0.1% crystal violet, and the number of migrated cells was determined under microscope.

Cell colony formation assay

CRC cells (500 cells/well) were seeded in 12-well plates and cultured for 10 days to generate colonies. The colonies were fixed for 30 min and stained with 0.1% crystal violet. The number of colonies was quantified.

Animal studies

All animal experiments performed in this study were approved by the Ethics Committee of the first affiliated hospital of Zhengzhou University (ZZU-LAC20240719[03]). All mice were housed under specific pathogen-free conditions.

For subcutaneous tumor model, 8-week-old Balb/c nude mice were anesthetized and subcutaneously injected with indicated CRC cells (1×10^6 cells/100 μ l PBS). Tumor volume was measured every 2 days and calculated. 21 days after injection, the mice were euthanized and the tumors were harvested, weighed and photographed. For the survival analysis of tumor-bearing mice, the tumor-bearing mice would be removed from the study (termination) when the tumor volume reached to 1.5 cm³.

For liver metastasis model, 8-week-old Balb/c-nude mice were anesthetized and intrasplenically injected with indicated CRC cells (1×10^6 cells/100 μ L PBS). The spleen was resected 5 min later. 2 weeks post injection, the mice were euthanized and the livers were isolated for counting visible metastatic foci. Histologically hematoxylin eosin (H&E)-staining was further applied to confirm the metastatic foci.

For lung metastasis model, 8-week-old Balb/c-nude mice were injected with indicated CRC cells via tail veins. 3 weeks post injection, the mice were euthanized and the lungs were isolated for counting visible metastatic foci. Histologically hematoxylin eosin (H&E)-staining was further applied to confirm the metastatic foci.

Immunohistochemistry staining

The colorectal cancer tissue microarray (HCoLA180Su21, OUTDO, Shanghai) containing 94 cases was purchased from Shanghai Outdo Biotechnology. Human CRC tissues or mice xenograft tumor tissues were fixed in 4% formaldehyde solution, embedded with paraffin, and sectioned. For immunohistochemical (IHC) staining, the sections were stained with primary antibodies against Ki67 (1:5000) or Caspase 3 (1:200), followed with HRP-conjugated secondary antibodies (Dako). 3,3'-diaminobenzidine (DAB, Dako) was used for chromogen development and hematoxylin for counterstain. IHC staining was scored based on the product of staining intensity. Human colorectal cancer specimens used in this study was approved by Human Ethics Committee of the first affiliated hospital of Zhengzhou university and written informed consents were obtained from all patients (2024-KY-2337).

Statistical analysis

All data were analyzed by GraphPad Prism 8.0 and shown as means \pm standard deviation (SD) or means \pm standard error of mean (SEM). Unpaired Student's t-tests were used to compare quantitative data between two groups. One-way ANOVA analysis was performed in multiple groups. Kaplan-Meier method was used to obtain survival curves. $P < 0.05$ was considered statistically significant.

Results

PTOV1 is upregulated in CRC and associated with poor clinical outcomes

To assess the clinical significance of PTOV1 in CRC, we analyzed its expression in a CRC tissue microarray. PTOV1 expression was found to be higher in CRC tissues ($n = 94$) compared to adjacent tissues ($n = 82$) and positively correlated with tumor stages according to the American Joint Committee on Cancer (AJCC) criteria (Fig. 1A-D). Kaplan-Meier analysis revealed that

elevated PTOV1 expression was significantly associated with shorter overall survival (OS) in CRC (Fig. 1E). The upregulated expression of PTOV1 in CRC tissues was confirmed by western blot and RT-PCR in paired CRC tissues and peritumoral tissues (Fig. 1F-H). We further evaluated the prognostic effects of PTOV1 in CRC from clinical databases. Consistently, PTOV1 expression was elevated in tumor tissues (compared to adjacent non-cancerous tissues) and metastasis lesions (compared to primary tumor) in TCGA and GSE81558 database, and positively associated with poor OS and relapse-free survival (RFS) of CRC patients (Fig. 1I-K; Figure S1A-D). These results suggest that PTOV1 may function as an oncogene in CRC progression.

PTOV1 promotes the proliferation, migration and invasion abilities of CRC cells in vitro

To explore the biological functions of PTOV1 in CRC, we performed gain- or loss- of function studies by stably overexpressing or knockdown PTOV1 in CRC cell lines. The efficiency of PTOV1 overexpression and knockdown were detected by western blot (Fig. 2A-B). We performed colony formation, CCK8 and EdU assays to evaluate the impact of PTOV1 on CRC cell growth and proliferation abilities. The results showed that PTOV1-overexpressing CRC cells had higher proliferation rate than control cells (Fig. 2C, E; Figure S2A, B, E). By contrast, the proliferation rate was remarkably reduced in PTOV1 stably knockdown cells (Fig. 2D, F; Figure S2C, D, F). Transwell assays showed that the cell migration and invasion abilities were also increased in PTOV1-overexpressing cells (Fig. 2G; Figure S2G) and decreased in PTOV1 silenced cells (Fig. 2H; Figure S2H). Moreover, PTOV1 up-regulated the mesenchymal markers (N-cadherin and vimentin) and proliferation related markers (c-MYC and CyclinD1), while down-regulated the epithelial marker (E-cadherin) in CRC cells (Fig. 2I-J). Collectively, these results demonstrate that PTOV1 promotes the proliferation, migration and invasion abilities of CRC cells.

PTOV1 promotes tumor growth and metastasis of CRC cells in vivo

We next examined the effect of PTOV1 on pathological progression of CRC in vivo. We established a xenograft model by subcutaneous injection of PTOV1 stably overexpression or knockdown CRC cells in nude mice. The tumor growth rate and tumor weight in the PTOV1 overexpression group were markedly increased compared to the control group (Fig. 3A-C). Conversely, knockdown of PTOV1 resulted in a decreased tumor growth rate and terminal tumor weight (Fig. 3D-F). Immunohistochemical staining showed that overexpression of PTOV1 upregulated the expression of proliferation marker Ki67 and downregulated the apoptosis related marker

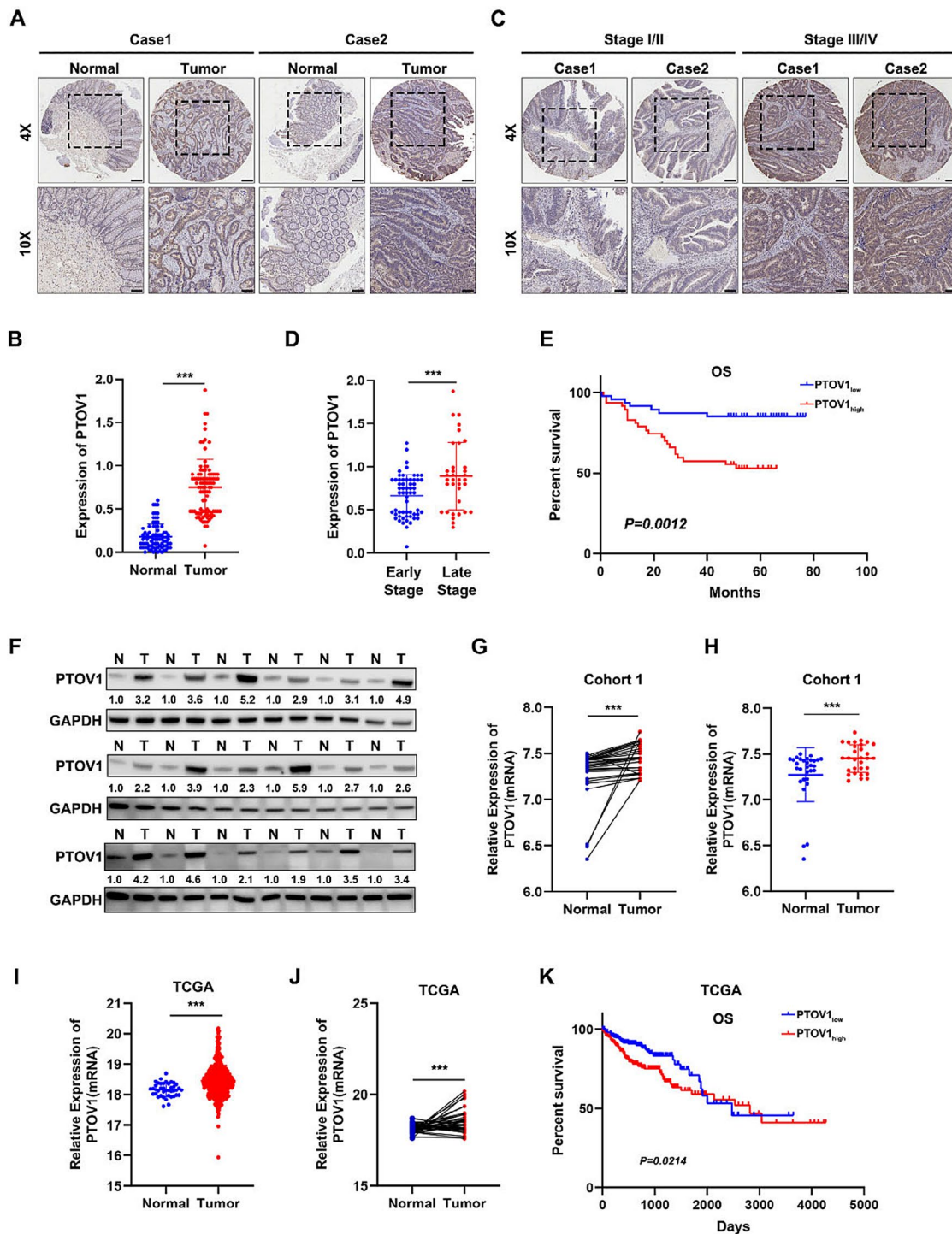


Fig. 1 PTOV1 is upregulated in CRC and correlated with unfavorable prognosis. **(A)** Representative images of PTOV1 immunohistochemistry staining in tumor ($n=94$) and adjacent normal tissues ($n=82$) in CRC tissue microarray. Scale bars, 200 μm for 5 x and 100 μm for 10 x magnification. **(B)** Quantification of mean density of PTOV1 staining in tissue microarray from **(A)**. $***, P < 0.001$. **(C)** Representative images of PTOV1 immunohistochemistry staining in early stage (stage I/II, $n=59$) tissues and late stage (stage III/IV, $n=35$) tissues in CRC tissue microarray. Scale bars, 200 μm for 5 x and 100 μm for 10 x magnification. **(D)** Quantification of mean density of PTOV1 staining in tissue microarray from **(C)**. $***, P < 0.001$. **(E)** Kaplan–Meier survival analysis of overall survival (OS) based on PTOV1 expression in CRC tissue microarray. $P=0.0012$. **(F)** Western blot analysis of PTOV1 expression in 18 paired CRC tissues and peritumoral tissues collected by us. **(G)** RT-PCR analysis of PTOV1 mRNA expression in 30 paired CRC tissues collected by us. $***, P < 0.001$. **(H)** RT-PCR analysis of PTOV1 mRNA expression in primary tumor and adjacent normal tissues collected by us. $***, P < 0.001$. **(I)** Analysis of PTOV1 mRNA expression in primary tumor ($n=453$) and adjacent normal tissues ($n=41$) in TCGA database. $***, P < 0.001$. **(J)** Analysis of PTOV1 mRNA expression in 41 paired CRC tissues in TCGA database. $***, P < 0.001$. **(K)** Kaplan–Meier survival analysis of overall survival (OS) based on PTOV1 expression in TCGA database. $P=0.0214$

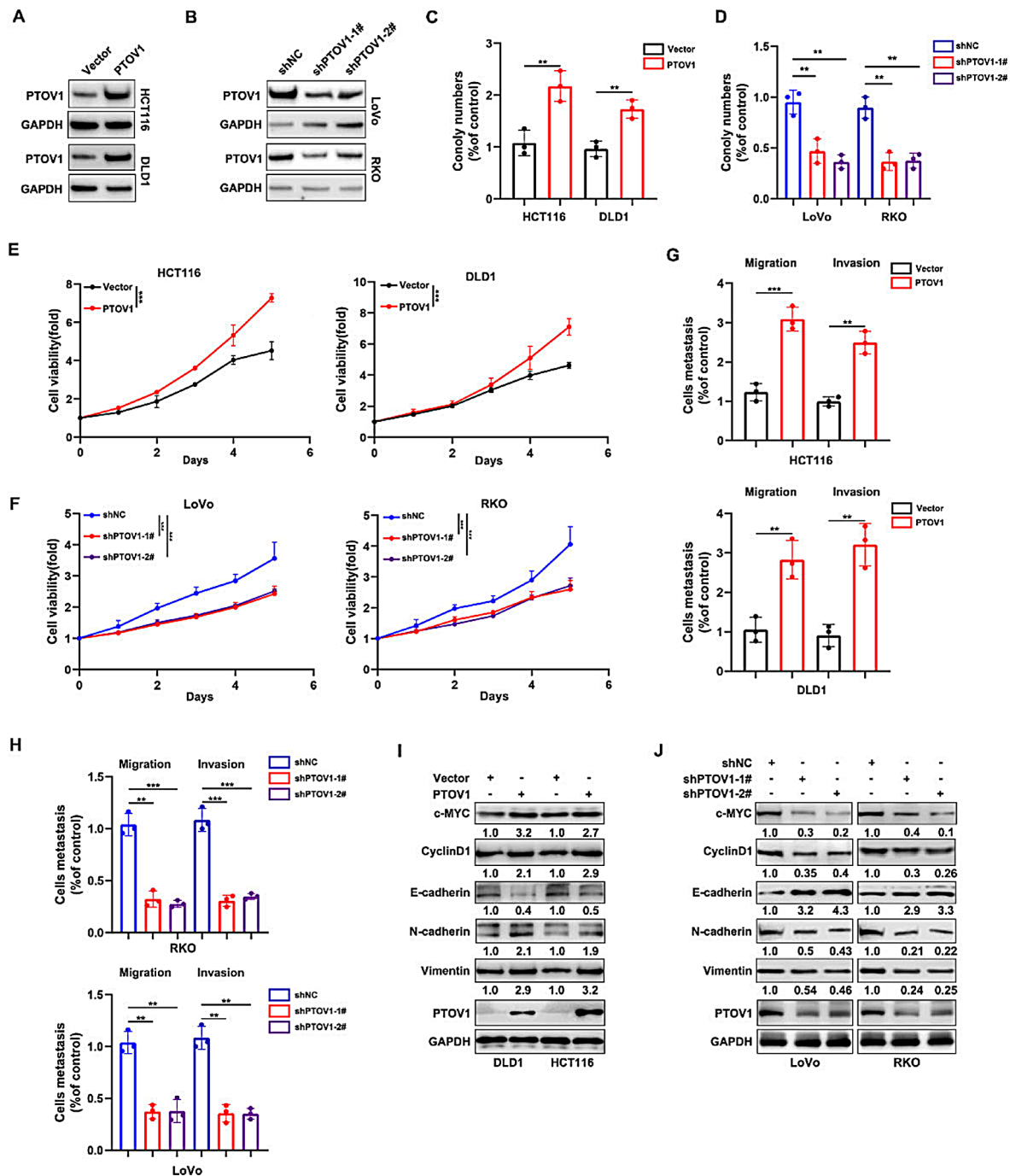


Fig. 2 PTOV1 promotes CRC progression in vitro. **(A)** Western blot analysis of PTOV1 expression in PTOV1 stably overexpression HCT116 and DLD1 cells. **(B)** Western blot analysis of PTOV1 expression in PTOV1 stably knockdown LoVo and RKO cells. **(C)** The colony formation assay of PTOV1 stably overexpression HCT116 and DLD1 cells. ***P* < 0.01. **(D)** The colony formation assay of PTOV1 stably knockdown LoVo and RKO cells. ***P* < 0.01. **(E)** The CCK8 assay of PTOV1 stably overexpression HCT116 (left panel) and DLD1 cells (right panel). ****P* < 0.001. **(F)** The CCK8 assay of PTOV1 stably knockdown LoVo (left panel) and RKO cells (right panel). ****P* < 0.001. **(G)** The migration and invasion assay of PTOV1 stably overexpression HCT116 (upper panel) and DLD1 cells (lower panel). The average number of cells per field were calculated. *n* = 3 samples per group, four fields per sample. ***P* < 0.01; ****P* < 0.001. **(H)** The migration and invasion assay of PTOV1 stably knockdown RKO (upper panel) and LoVo cells (lower panel). The average number of cells per field were calculated. *n* = 3 samples per group, four fields per sample. ***P* < 0.01; ****P* < 0.001. **(I)** Western blot analysis of c-MYC, CyclinD1, N-cadherin, E-cadherin, and Vimentin expression in PTOV1 stably overexpression HCT116 and DLD1 cells. **(J)** Western blot analysis of c-MYC, CyclinD1, N-cadherin, E-cadherin, and Vimentin expression in PTOV1 stably knockdown LoVo and RKO cells

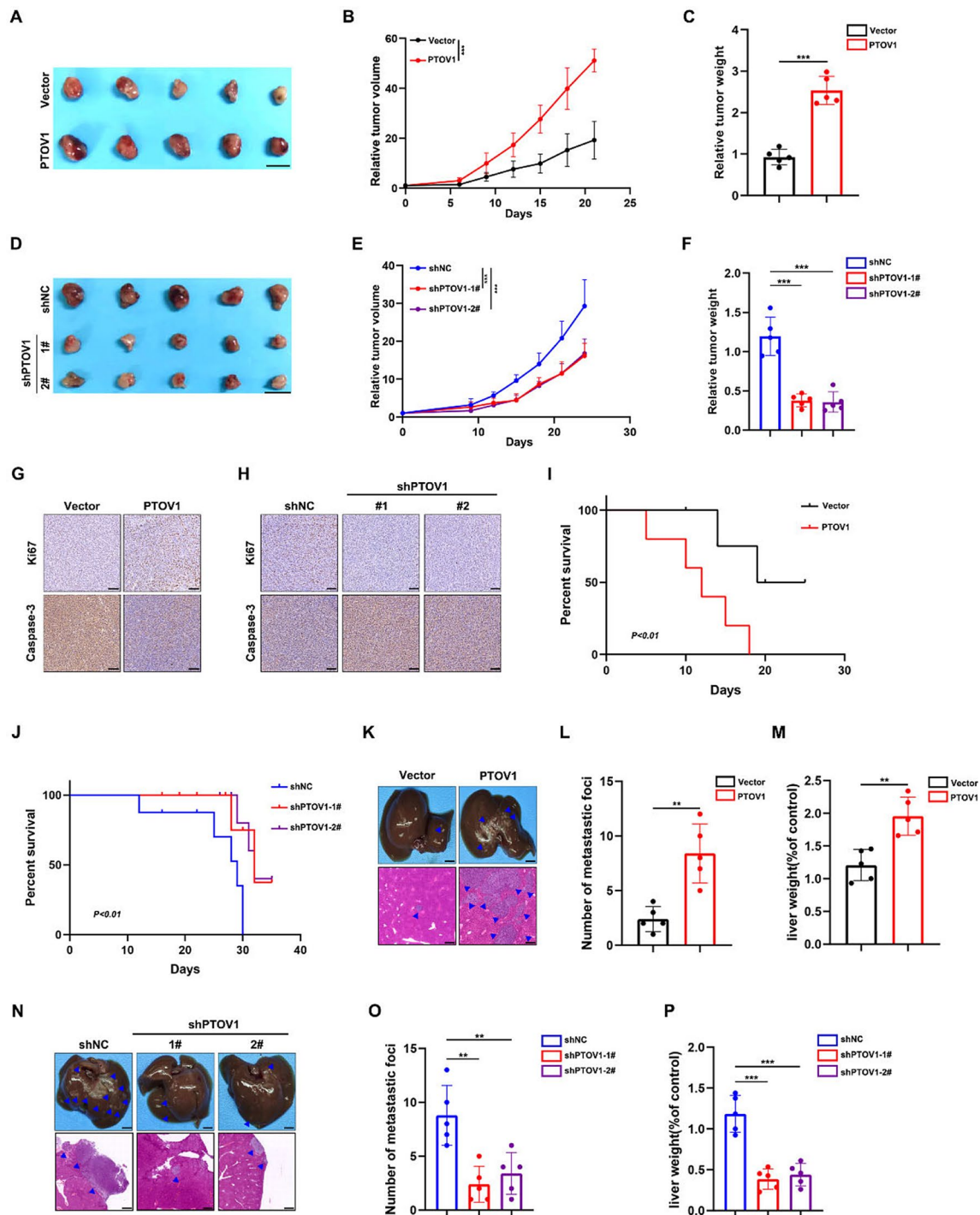


Fig. 3 PTOV1 promotes CRC progression in vivo. **(A-C)** PTOV1 stably overexpression or control HCT116 cells were subcutaneously injected into nude mice. Representative tumor sizes **(A)**, tumor growth curves **(B)**, and tumor weight **(C)** are shown. $n=5$ per group; Scale bar, 50 mm. ***, $P < 0.001$. **(D-F)** PTOV1 stably knockdown or control LoVo cells were subcutaneously injected into nude mice. Representative tumor sizes **(D)**, tumor growth curves **(E)**, and tumor weight **(F)** are shown. $n=5$ per group; Scale bar, 50 mm. ***, $P < 0.001$. **(G-H)** The representative immunohistochemical staining of Ki67 and Caspase-3 in xenograft tumor from PTOV1 stably overexpression **(G)** or PTOV1 stably knockdown **(H)** groups. Scale bar, 100 μm . **(I)** Kaplan–Meier analysis of tumor-bearing nude mice with subcutaneous injected with PTOV1 stably overexpression and control HCT116 cells. $P < 0.01$. **(J)** Kaplan–Meier analysis of tumor-bearing nude mice with subcutaneous injected with PTOV1 stably knockdown and control LoVo cells. $P < 0.01$. **(K-M)** PTOV1 stably overexpression and control HCT116 cells were injected into nude mice via spleen. The representative hematoxylin and eosin (H&E) images **(K)**, quantification of metastatic foci **(L)** and liver weight **(M)** were shown. $n=5$ per group. Scale bars **(K, upper panel)**, 1 cm; Scale bars **(K, lower panel)**, 100 μm . **, $P < 0.01$. **(N-P)** PTOV1 stably knockdown and control LoVo cells were injected into nude mice via spleen. The representative hematoxylin and eosin (H&E) images **(N)**, quantification of metastatic foci **(O)** and liver weight **(P)** were shown. $n=5$ per group. Scale bars **(N, upper panel)**, 1 cm; Scale bars **(N, lower panel)**, 100 μm . **, $P < 0.01$; ***, $P < 0.001$

Caspase-3, whereas PTOV1 knockdown had the opposite effects (Fig. 3G-H). Moreover, the survival rate was lower in PTOV1 overexpression group and higher in PTOV1 knockdown group than that of the control groups (Fig. 3I-J). To validate the results that PTOV1 promoted migration and invasion of CRC cells in vitro, we constructed lung and liver metastasis mouse model by tail-vein or spleen injection of CRC cells. The results showed that PTOV1 overexpression significantly promoted the lung and liver metastasis (Fig. 3K-M, Figure S3A-C) while PTOV1 knockdown suppressed the metastasis in vivo (Fig. 3N-P). Altogether, these data indicate that PTOV1 facilitates tumor growth and metastasis of CRC cells in vivo.

p53 is a binding partner of PTOV1

To gain insight into the molecular mechanism underlying the oncogenic effect of PTOV1 in CRC, we performed an immunoprecipitation-coupled mass spectrometry screening (Fig. 4A). Interestingly, p53 was identified as a potential interacting partner of PTOV1 (Fig. 4B). PTOV1 and p53 exhibited marked colocalization in the nucleus (Fig. 4C), and their physical interaction was confirmed by reciprocal co-immunoprecipitation (Co-IP) experiments (Fig. 4D). To determine the functional domain of p53 that bound to PTOV1, we generated a series of p53 truncations and performed the Co-IP experiments with PTOV1 (Fig. 4E). The result showed that full length p53 and its truncated forms with the central DNA binding (p53C) domain mediating the binding of p53 to DNA [18], could interact with PTOV1, while the truncations lacking p53C domain completely abolished the interaction (Fig. 4G). PTOV1 mainly contains two highly homologous domains (66% identity) identified as A domain (146 amino acids) and B domain (143 amino acids) [19] (Fig. 4F). To determine which domain was responsible for the interaction with p53, we co-immunoprecipitated p53 with either full length PTOV1 or the truncated forms (PTOV1₁₋₂₃₄ and PTOV1₂₅₃₋₄₁₆) and found that the truncation (PTOV1₁₋₂₃₄) containing A domain was able to interact with p53 (Fig. 4H). We also investigated the effects of PTOV1₁₋₂₃₄ on CRC progression. The results showed that PTOV1₁₋₂₃₄ was able to promote cell proliferation, migration and invasion in CRC (Figure S4A-F).

PTOV1 promotes the degradation of p53 by autophagy

We next wondered whether the expression of PTOV1 or p53 was affected by their interactions. Western blot assay showed that overexpression of PTOV1 decreased p53 protein levels in CRC cell lines (Fig. 5A). We transfected CRC cells with increasing amount of PTOV1 plasmid and found that the protein levels of p53 were markedly decreased with increasing PTOV1 plasmid concentration (Fig. 5B, Figure S5A). Conversely, the accumulation

of p53 was observed upon PTOV1 knockdown in CRC cells (Fig. 5C). The cycloheximide chase assay showed that overexpression of PTOV1 significantly accelerated p53 protein degradation (Fig. 5, Figure S5B). To determine the degradation pathways of p53 upon PTOV1 overexpression, we treated the control or PTOV1 overexpression cells with the proteasome inhibitor MG132 or autophagy inhibitor Chloroquine (CQ). Of note, the negative regulation of p53 by PTOV1 overexpression could be restored by CQ, but not the proteasome inhibitor MG132, suggesting that PTOV1 promotes the degradation of p53 by autophagy (Fig. 5E-F, Figure S5C-D). Moreover, inhibiting autophagy by ULK1 or ATG7 siRNAs, as well as with wortmannin, also reversed PTOV1's negative regulation of p53 (Fig. 5G-H, Figure S5E). Transmission electron microscopy (TEM) analysis showed that PTOV1-overexpressing cells displayed more autophagosome-like structures than control cells (Fig. 5I). PTOV1 overexpression also increased the number of GFP-LC3B puncta, enhanced endogenous LC3B-II accumulation and decreased SQSTM1/p62 protein levels, suggesting that autophagy was activated upon PTOV1 overexpression (Fig. 5J, Figure S5F-G). Consistently, PTOV1 knockdown could efficiently suppress autophagy (Fig. 5K). To further demonstrate PTOV1's effect on autophagic flux, we utilized the GFP-mCherry-LC3B plasmid that expressed green and red fluorescence proteins simultaneously to label autophagosomes and autophagosomes-lysosomes with red and yellow fluorescence, respectively [20]. PTOV1 overexpression increased the number of both autophagosomes and autophagosomes-lysosomes in HCT116 cells (Fig. 5L). Collectively, these results indicate that PTOV1 promotes the autophagic degradation of p53 in CRC cells.

PTOV1 promotes CRC progression via decreasing p53 expression

To determine whether p53 was involved in PTOV1's modulation on CRC progression, we performed functional rescue experiments in PTOV1 stably overexpression CRC cells. Overexpression of p53 substantially abrogated the enhanced cell proliferation and metastasis abilities in PTOV1 overexpressed CRC cells in vitro, as well as the regulation of the EMT markers (E-cadherin, N-cadherin and Vimentin) and proliferation related markers (c-MYC and CyclinD1) (Fig. 6A-C; Figure S6A-F). p53 overexpression also reversed the increased tumor volumes and weights induced by PTOV1 overexpression in subcutaneous tumor model (Fig. 6D-F). Immunohistochemical staining showed that the upregulation of Ki67 and downregulation of Caspase-3 in PTOV1 overexpression group were abolished upon p53 overexpression (Fig. 6G). These data demonstrated that PTOV1 promoted CRC progression through decreasing p53

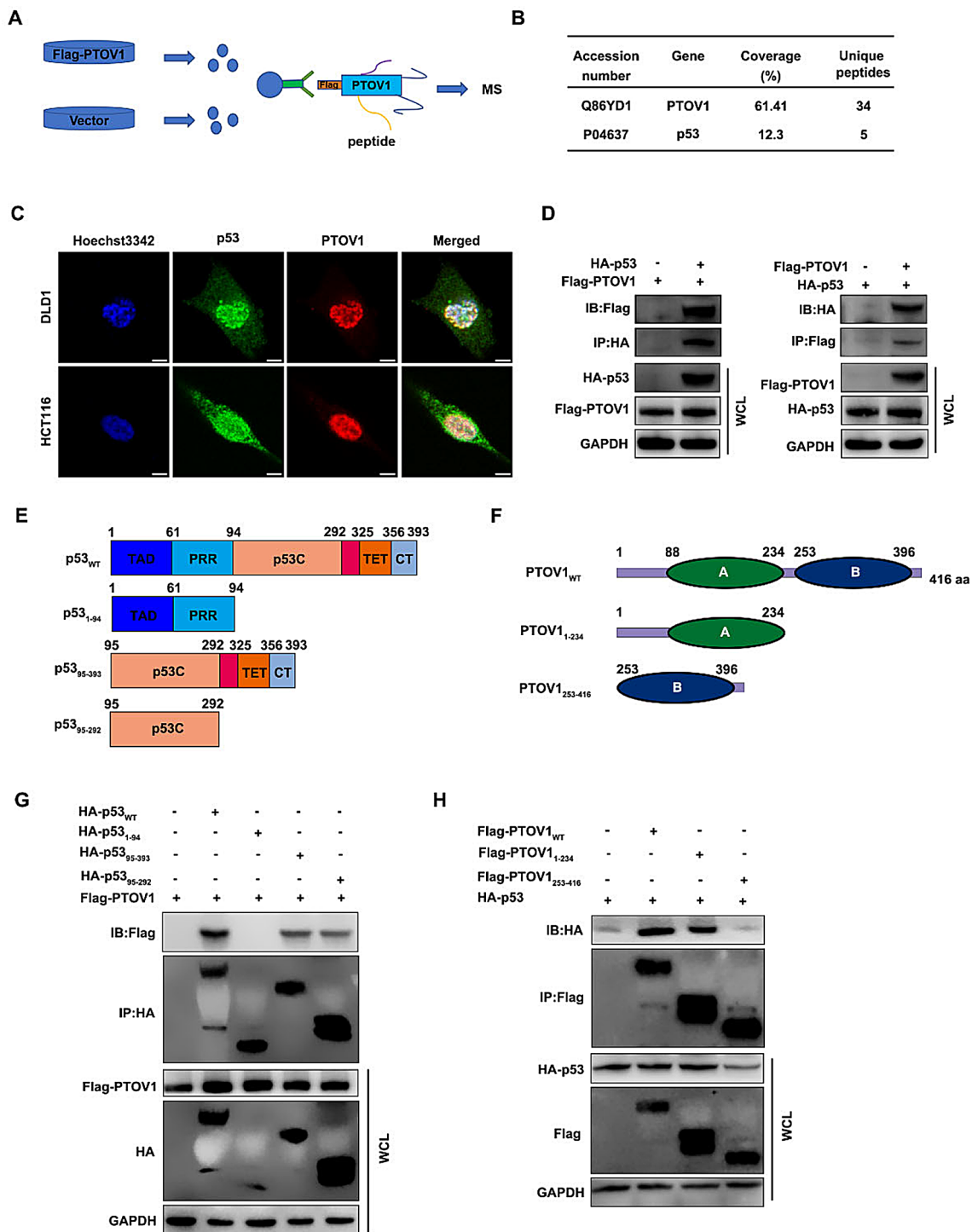


Fig. 4 PTOV1 binds to p53. **(A)** The schematic diagram of the screening for PTOV1 interacting proteins. **(B)** HCT116 cells were transfected with empty vector or Flag-PTOV1. Cell lysates were immunoprecipitated with anti-FLAG antibody. p53 was identified via mass spectrometry. **(C)** Immunofluorescence assay of PTOV1 and p53 in DLD1 or HCT116 cells. Representative confocal microscopy images were shown. Scale bars, 5 μ m. **(D)** HCT116 cells were co-transfected with Flag-PTOV1 and HA-p53 for 48 h. Total cell lysates were immunoprecipitated with anti-Flag or anti-HA antibodies. HA-p53 and Flag-PTOV1 were detected by western blot. **(E-F)** The schematic diagram of full-length and mutants of p53 **(E)** and PTOV1 **(F)**. **(G)** HCT116 cells were co-transfected with HA-p53, HA-p53₁₋₉₄, HA-p53₉₅₋₃₉₃, HA-p53₉₅₋₂₉₂ and Flag-PTOV1 for 48 h. Total cell lysates were immunoprecipitated with anti-HA antibody. Immunoprecipitation complex was detected by anti-HA and anti-Flag antibodies. **(H)** HCT116 cells were co-transfected with Flag-PTOV1, Flag-PTOV1₁₋₂₃₄, Flag-PTOV1₂₅₃₋₄₁₆ and HA-p53 for 48 h. Total cell lysates were immunoprecipitated with anti-Flag antibody. Immunoprecipitation complex was detected by western blot with anti-HA and anti-Flag antibodies

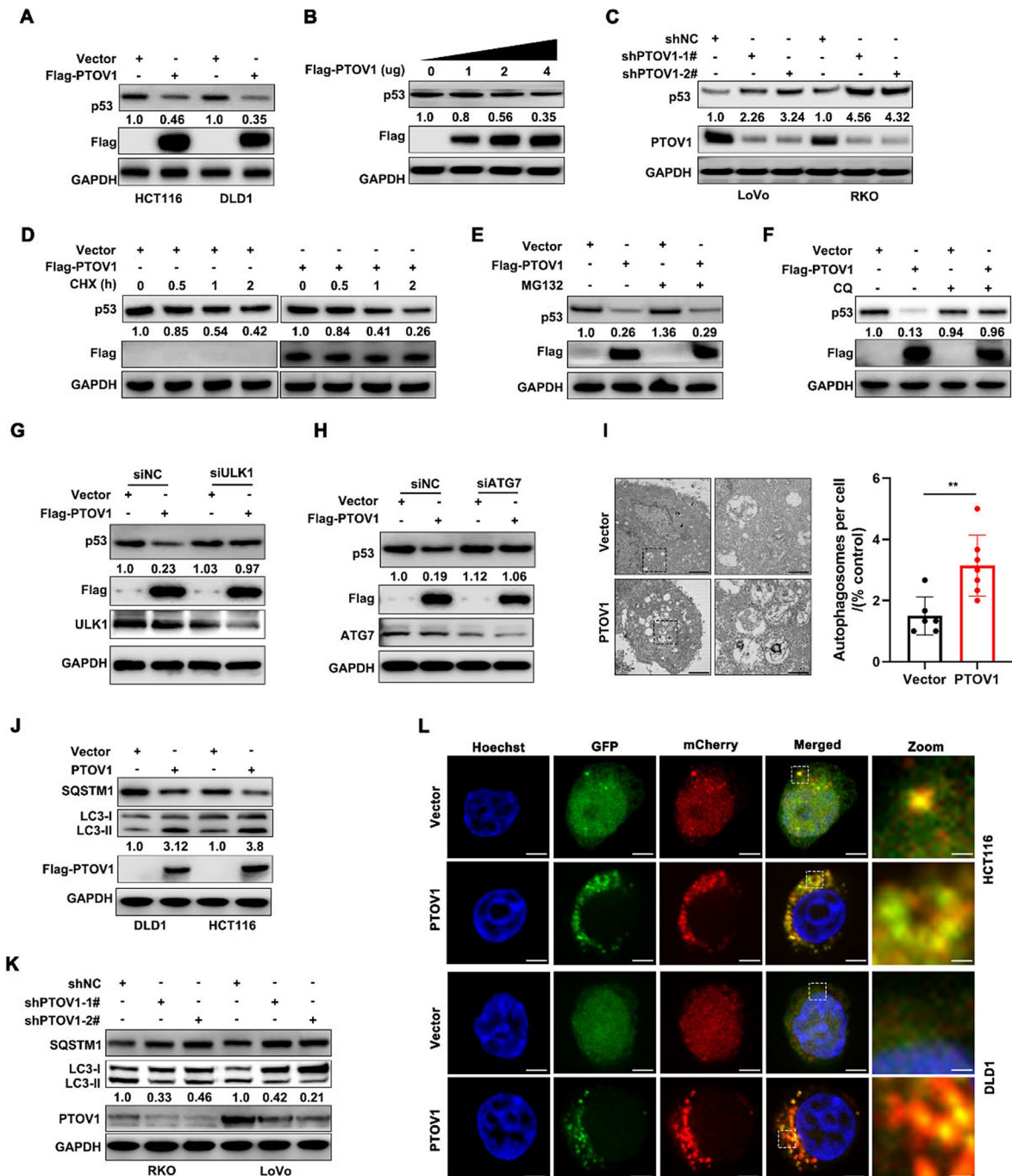


Fig. 5 POTV1 promotes the autophagic degradation of p53. **(A)** Western blot analysis of p53 expression in PTOV1 stably overexpression HCT116 and DLD1 cells. **(B)** Western blot analysis of p53 expression in HCT116 cells transfected with indicated amount of Flag-PTOV1 plasmid for 48 h. **(C)** Western blot analysis of p53 expression in PTOV1 stably knockdown LoVo and RKO cells. **(D)** Cycloheximide chase analysis of p53 protein half-life in PTOV1 stably overexpression HCT116 and DLD1 cells treated with 10 μ M cycloheximide. **(E-F)** Western blot analysis of p53 expression in PTOV1 stably overexpression HCT116 cells treated with 10 μ M MG132 for 12 h **(E)** or 50 μ M CQ for 4 h **(F)**. **(G-H)** PTOV1 stably overexpression HCT116 cells were transfected with siULK1 **(G)** or siATG7 **(H)** for 48 h, western blot analysis of p53 protein levels. **(I)** TEM analysis of PTOV1 stably overexpression HCT116 cells and representative TEM images were shown. The number of autophagic structures per cell was quantified. Scale bar, 2 μ m; **, $P < 0.01$. **(J)** Western blot analysis of LC3 and SQSTM1 protein levels in PTOV1 stably overexpression HCT116 and DLD1 cells. **(K)** Western blot analysis of LC3 and SQSTM1 protein levels in PTOV1 stably knockdown LoVo and RKO cells. **(L)** PTOV1 stably overexpression HCT116 or DLD1 cells were transfected with GFP-mCherry-LC3B for 48 h. GFP-mCherry-LC3B distribution was observed by confocal microscopy. Scale bar, 5 μ m

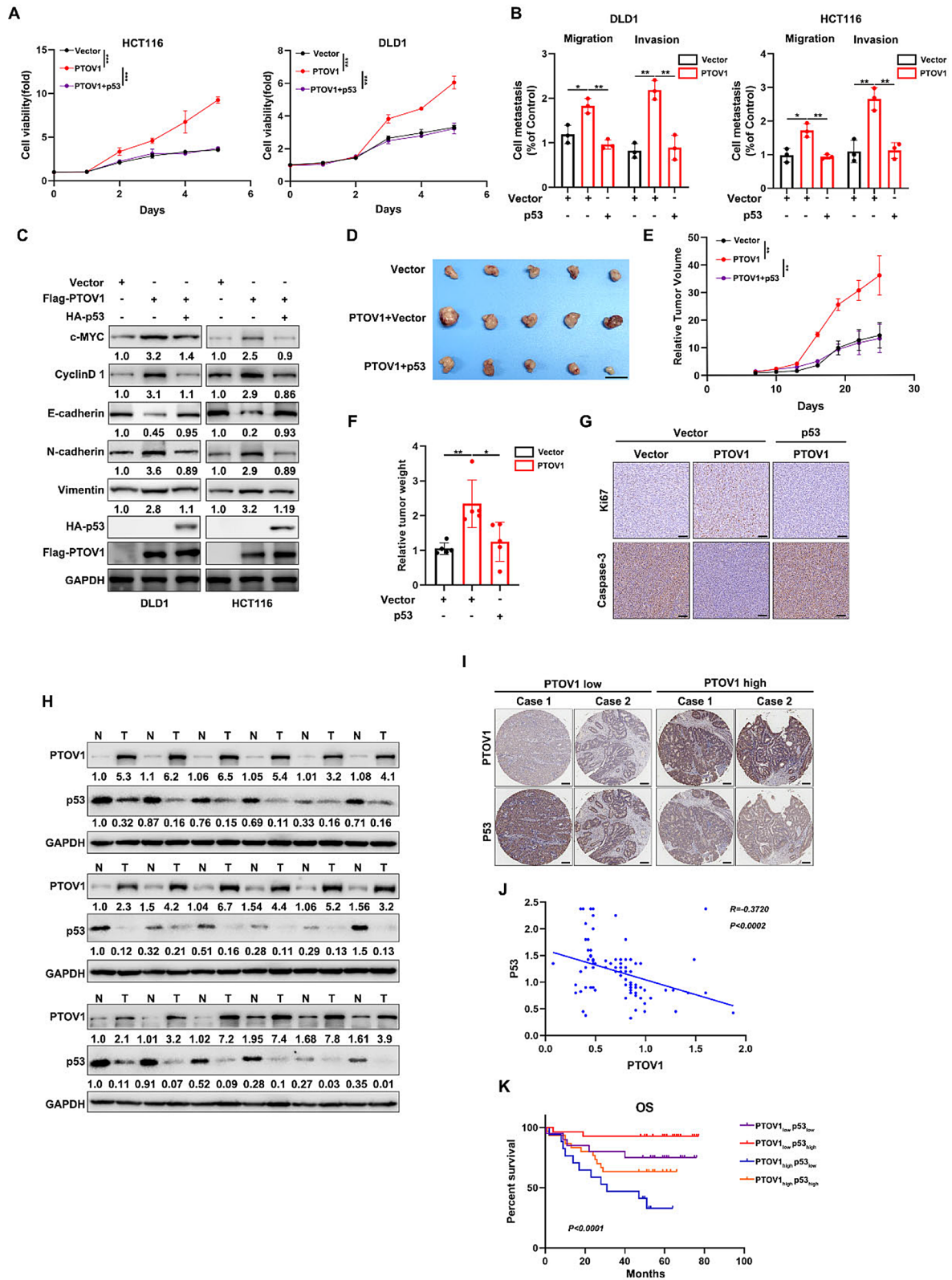


Fig. 6 (See legend on next page.)

(See figure on previous page.)

Fig. 6 PTOV1 facilitates CRC progression through downregulating p53. **(A)** The CCK8 assay of PTOV1 stably overexpression HCT116 and DLD1 cells with or without p53 overexpression. **(B)** The migration and invasion assay of PTOV1 stably overexpression LoVo and RKO cells with or without p53 overexpression. The average number of cells per field were calculated. $n=3$ samples per group, four fields per sample. *, $P<0.05$; ***, $P<0.01$. **(C)** Western blot analysis of c-MYC, CyclinD1, N-cadherin, E-cadherin and Vimentin expression in PTOV1 stably overexpression HCT116 and DLD1 cells with or without p53 overexpression. **(D-F)** PTOV1 stably overexpression or control HCT116 cells with or without p53 overexpression were subcutaneously injected into nude mice. Representative tumor sizes **(D)**, tumor growth curves **(E)**, and tumor weight **(F)** are shown. $n=5$ per group; Scale bar, 50 mm. ***, $P<0.001$. **(G)** The representative immunohistochemical staining of Ki67 and Caspase-3 in xenograft tumor from PTOV1 stably overexpression with or without p53 overexpression groups. Scale bar, 100 μm . **(H)** Western blot analysis of PTOV1 and p53 expression in 18 paired CRC tissues and peritumoral tissues. **(I)** Representative images of PTOV1 and p53 immunohistochemistry staining in tumor ($n=94$) and adjacent normal tissues ($n=82$) in CRC tissue microarray. Scale bars, 200 μm for 5 x and 100 μm for 10 x magnification. **(J)** Pearson correlation analysis of PTOV1 and p53 expression in CRC tissue microarray. $P<0.002$. **(K)** Kaplan–Meier survival analysis of overall survival (OS) based on PTOV1 and p53 expression in CRC tissue microarray. $P<0.0001$

expression. Previous studies showed that PTOV1 promoted tumor progression in CRC and breast cancer through activating AKT1 signaling pathway and WNT pathway [21, 22]. To determine p53-independent pathways affected by PTOV1, we analyzed these two well-established oncogenic pathways in CRC. The results showed that PTOV1 overexpression indeed facilitated the activation of Wnt/ β -catenin, and PI3K-AKT pathways (Figure S7A-B). Moreover, the antagonists of these pathways by specific inhibitor could inhibit the pro-oncogenic phenotypes induced by PTOV1 overexpression (Figure S7C-F).

We next investigated the clinical relevance between PTOV1 and p53 in CRC. Western blot and CRC tissue microarray assays demonstrated that PTOV1 expression was inversely related to p53 expression (Fig. 6H-J). Moreover, patients with high levels of PTOV1 and low levels of p53 (PTOV1^{high}p53^{low}) had the worst prognosis, whereas the PTOV1^{low}p53^{high} patients had the best outcomes (Fig. 6K).

The autophagy cargo protein SQSTM1 drives p53 for autophagic degradation

The selective autophagic degradation of proteins is mediated by specific autophagy cargo receptor [23]. To identify which receptor is involved in the degradation of p53, we performed co-immunoprecipitation (Co-IP) experiments in HCT116 cells co-transfected with HA-p53 and several known autophagy cargo receptors. Among these autophagy receptors, only SQSTM1 significantly interacted with p53, implying that SQSTM1 might mediate the selective autophagic degradation of p53 (Fig. 7A). The interaction between SQSTM1 and p53 was confirmed by reciprocal co-immunoprecipitation (Co-IP) experiments (Fig. 7B-C). PTOV1 overexpression enhanced the interaction between p53 and SQSTM1 while PTOV1 knockdown impaired their interaction (Fig. 7D-E). Moreover, Knockdown of SQSTM1 rescued the decreased p53 protein levels induced by PTOV1 overexpression (Fig. 7F). p53 exhibited punctate cytoplasmic distribution and colocalized with SQSTM1 in the cytoplasm upon PTOV1 overexpression (Fig. 7G). These data indicate that PTOV1

overexpression promotes the interaction between p53 and SQSTM1, leading to p53 degradation by autophagy.

Knockdown of SQSTM1 inhibits the oncogenic effect of PTOV1 in CRC

Since SQSTM1 drives p53 for PTOV1 induced autophagic degradation, we wondered whether SQSTM1 knockdown inhibited the oncogenic effect of PTOV1 in CRC. Similar to the phenotype that p53 overexpression reversed the pro-tumor ability of PTOV1 in CRC, SQSTM1 knockdown abolished the enhanced cell proliferation and metastasis in PTOV1 overexpressed CRC cells in vitro and in vivo (Fig. 8A-G; Figure S8A-D), as well as the regulation of PTOV1 on the EMT markers (E-cadherin, N-cadherin and Vimentin), proliferation related markers (Ki67, c-MYC and CyclinD1) and apoptosis related marker (Caspase-3) (Fig. 8H-I). These data demonstrated that PTOV1 promoted CRC progression in a SQSTM1 dependent manner.

Discussion

PTOV1 is upregulated and associated with poor prognosis in various types of cancers, such as prostate cancer, breast cancer and non-small cell lung cancer, making it to be a potential target for cancer diagnosis and treatment [24–26]. However, the clinical significance and functional roles of PTOV1 in CRC remain unexplored. Our research group identified that PTOV1 was significantly upregulated in liver metastatic foci compared to primary CRC cells through RNA-seq analysis in a CRC liver metastasis mouse model (Data not shown). We analyzed the clinical relevance of PTOV1 in CRC cohorts from clinical databases, clinical specimens and commercial TMA. All these data showed that PTOV1 was upregulated in CRC tissues and significantly associated with unfavorable prognosis of CRC patients. Functional study demonstrated that PTOV1 was able to promote CRC progression in vitro and in vivo. Therefore, our study strongly supports PTOV1 as an oncogene in CRC.

Several studies have reported the potential molecular mechanisms by which PTOV1 promotes tumor progression. PTOV1 overexpression recruited HDACs to the promoter of DDK1, reduced DKK1 promoter histone

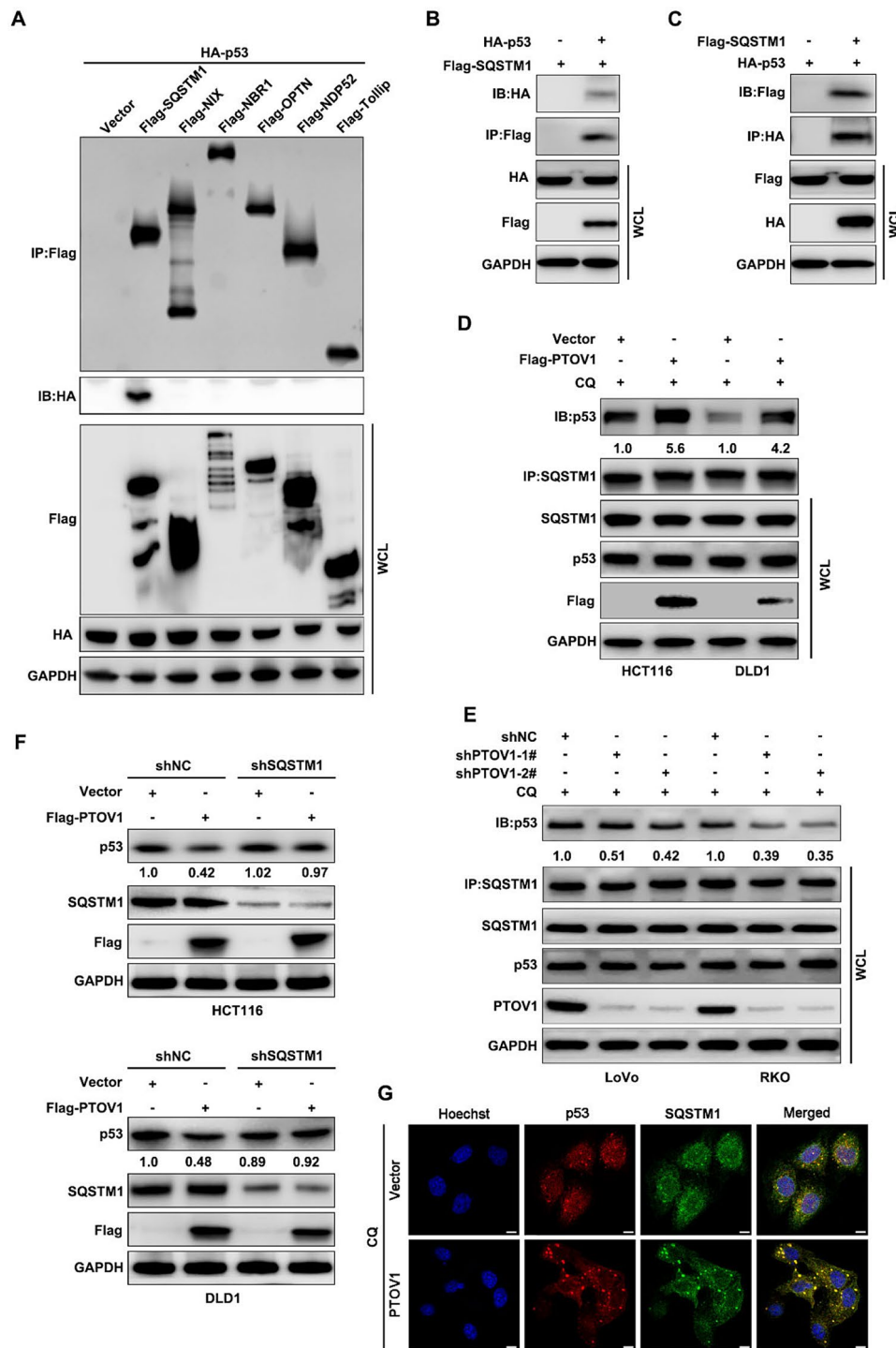


Fig. 7 PTOV1 promotes p53 autophagic degradation dependent on SQSTM1. **(A)** HCT116 cells were co-transfected with indicated autophagy cargo receptors and HA-p53 for 48 h. Total cell lysates were immunoprecipitated with anti-Flag antibody. Immunoprecipitation complex was detected by anti-HA and anti-Flag antibodies. **(B-C)** HCT116 cells were co-transfected with Flag-SQSTM1 and HA-p53 for 48 h. Total cell lysates were immunoprecipitated with anti-Flag **(B)** or anti-HA **(C)** antibodies. HA-p53 and Flag-SQSTM1 were detected by western blot. **(D)** PTOV1 stably overexpression HCT116 and DLD1 cells or control cells were treated with CQ (50µM) for 4 h. Total cell lysates were immunoprecipitated with anti-SQSTM1 antibodies. p53 and SQSTM1 were detected by western blot. **(E)** PTOV1 stably knockdown LoVo and RKO cells or control cells were treated with CQ (50µM) for 4 h. Total cell lysates were immunoprecipitated with anti-SQSTM1 antibodies. p53 and SQSTM1 were detected by western blot. **(F)** PTOV1 stably overexpression HCT116 and DLD1 cells were infected with SQSTM1 shRNA for 48 h. Western blot analysis of p53 and SQSTM1 protein levels. **(G)** Immunofluorescence assay of p53 and SQSTM1 in PTOV1 stably overexpression HCT116 and cells treated with CQ (50µM) for 4 h. Representative confocal microscopy images were shown. Scale bars, 5 µm

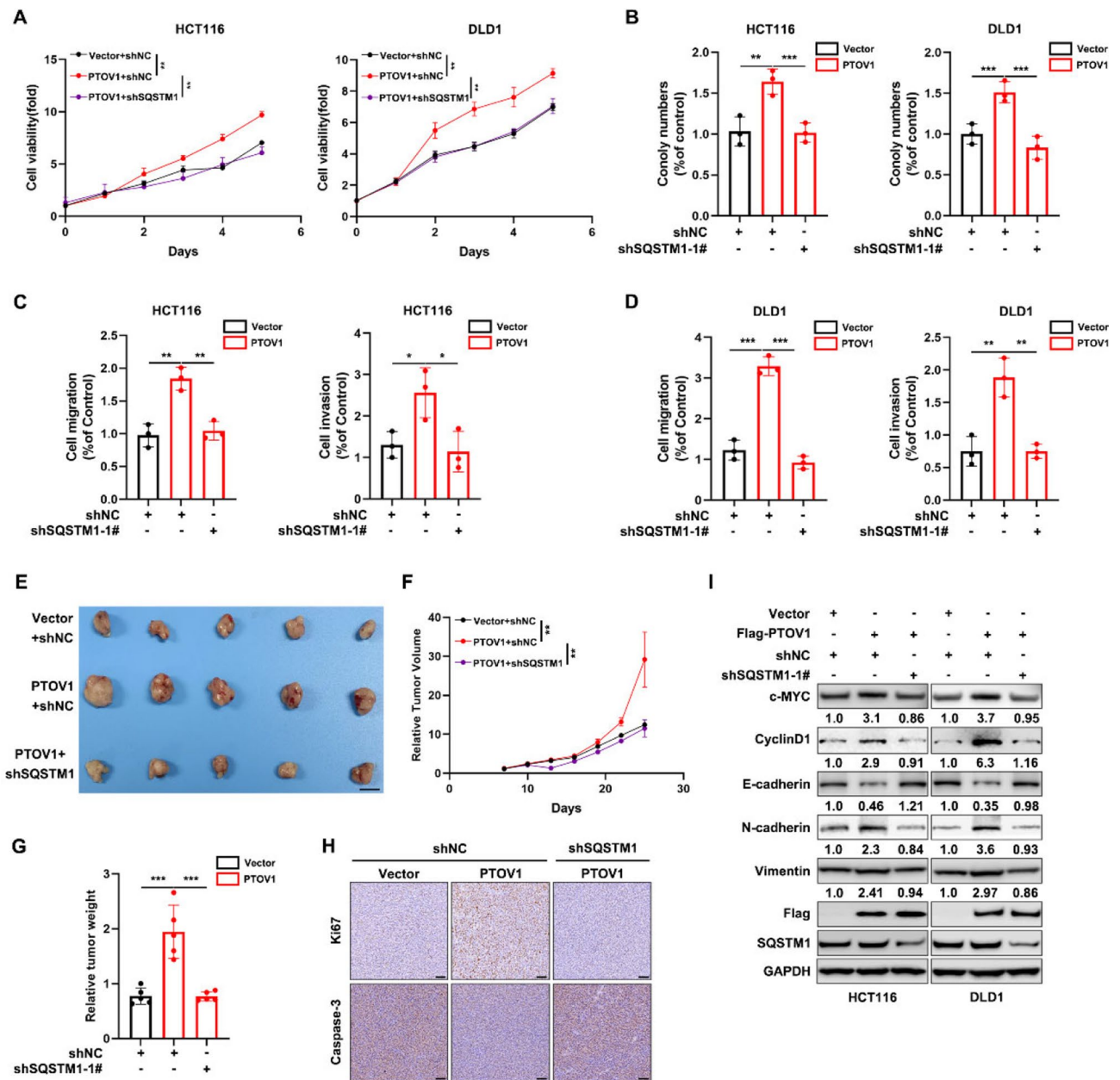


Fig. 8 PTOV1 promoted CRC progression in a SQSTM1 dependent manner. **(A)** The CCK8 assay of PTOV1 stably overexpression HCT116 and DLD1 cells with or without SQSTM1 knockdown. **, $P < 0.01$. **(B)** The colony formation assay of PTOV1 stably overexpression HCT116 and DLD1 cells with or without SQSTM1 knockdown. **, $P < 0.01$; ***, $P < 0.001$. **(C-D)** The migration and invasion assay of PTOV1 stably overexpression HCT116 **(C)** and DLD1 **(D)** cells with or without SQSTM1 knockdown. The average number of cells per field were calculated. $n = 3$ samples per group, four fields per sample. *, $P < 0.05$; ***, $P < 0.01$. **(E-G)** PTOV1 stably overexpression or control HCT116 cells with or without SQSTM1 knockdown were subcutaneously injected into nude mice. Representative tumor sizes **(E)**, tumor weight **(F)**, and tumor growth curves **(G)** are shown. $n = 5$ per group; Scale bar, 50 mm. ***, $P < 0.001$. **(H)** The representative immunohistochemical staining of Ki67 and Caspase-3 in xenograft tumor from PTOV1 stably overexpression with or without SQSTM1 knockdown groups. Scale bar, 100 μm . **(I)** Western blot analysis of c-MYC, CyclinD1, N-cadherin, E-cadherin and Vimentin expression in PTOV1 stably overexpression HCT116 and DLD1 cells with or without SQSTM1 knockdown

acetylation and repressed DKK1 transcription [22]. PTOV1 could interact with RACK1 and stimulate the protein synthesis of c-Jun, thus promoted the epithelial-mesenchymal-transition (EMT) of prostate cancer cells [27]. Here, we found that PTOV1 interacted with p53 and impaired its protein stability. The oncogenic ability of

PTOV1 in CRC was largely dependent on the downregulation of p53. PTOV1 contains two highly homologous domains identified as A domain (PTOV1) and B domain (PTOV1). Interestingly, unlike previous studies reported that PTOV1 interacted with RACK1 and Flotillin-1 through its B domain [27, 28], A domain is necessary

for the binding of PTOV1 and p53, suggesting that the two domains may have distinct functions. More importantly, PTOV1-mediated regulation of p53 was observed in clinical samples, as there was a negative correlation between the expression of PTOV1 and p53 in CRC tissues. PTOV1 and p53 were clinically related in predicting survival of CRC patients. Our findings may suggest a novel combination strategy of targeting the PTOV1–p53 axis for CRC treatment.

The regulation of p53 stability is a pivotal concern in cancer research. p53 is subject to degradation through both the autophagy-lysosome and the proteasome pathways [29–31]. Although the proteasome-mediated degradation of p53 has been well-documented, studies focusing on p53 degradation via autophagy are comparatively sparse. Initial findings revealed that p53 could be degraded through chaperone-mediated autophagy (CMA) or MDM2-mediated autophagic degradation [32]. Another research showed that Sunitinib, a small molecule multi kinase inhibitor, induced autophagic degradation of wild type p53 proteins in cancer cells [33]. Our studies identified PTOV1 as a key upstream modulator of autophagic degradation of p53. Blocking autophagy markedly mitigates the p53 degradation triggered by PTOV1 overexpression.

The selective autophagic degradation of substrate proteins require the mediation of autophagy receptor proteins [34]. We found that SQSTM1 served as the receptor protein involved in the PTOV1-mediated selective autophagic degradation of p53. Previous studies reported that SQSTM1 functions as an oncogene through inhibiting apoptosis and promoting cell proliferation in CRC [35, 36]. Our study showed that knockdown of SQSTM1 could reverse the decreased p53 protein levels and the oncogenic phenotypes induced by PTOV1 overexpression. These results suggest that targeting the SQSTM1-mediated selective autophagy pathway may offer new therapeutic strategy for CRC patients with high PTOV1 expression.

Several limitations warrant acknowledgment [37, 38]. Firstly, in vitro and animal models may not fully capture the complexity of human CRC, potentially limiting the applicability of the findings for clinical application. Secondly, the human sample size in this study is limited, and further validation in larger clinical cohorts is essential. Finally, the exact mechanisms by which PTOV1 influences autophagy are not yet understood, representing a promising direction for future research.

Conclusion

In summary, we demonstrate for the first time that PTOV1 facilitates CRC progression through promoting SQSTM1-mediated autophagic degradation of p53. Our findings underscore the oncogenic roles of PTOV1

in CRC, contribute to the understanding of p53 stability regulation by autophagy, and highlight the high clinical correlation between PTOV1 and p53 in CRC. The work supports the potentiality for exploration of PTOV1–SQSTM1–p53 axis for CRC therapy.

Abbreviations

CRC	Colorectal Cancer
PTOV1	Prostate Tumor Overexpressed 1
IP	Immunoprecipitation
ATCC	American Type Culture Collection
LC-MS	Liquid chromatograph-mass spectrometry
TEM	Transmission electron microscopy
AJCC	American Joint Committee on Cancer
OS	Overall survival
RFS	Relapse-free survival
CMA	Chaperone-mediated autophagy

Supplementary Information

The online version contains supplementary material available at <https://doi.org/10.1186/s12967-025-06179-x>.

Supplementary Material 1

Acknowledgements

We thank Yuan Cao and Piao Zou at Analytical & Testing Center, Wuhan University of Science and Technology for their assistance in the experiments.

Author contributions

Zhibo Liu, Huifen Wang, and Di Wang designed research; Yongli Fan, Yuqin Li, Xia Luo, Shiqi Xiang, Jingchun Zhang, Weilong Chang, Rui Deng, Xianwen Ran, Yize Zhang, Yudie Cai, Weiwei Zhu performed research; Huifen Wang, and Yongli Fan analyzed data; Jia Hu and Zhibo Liu wrote the paper; Jia Hu and Di Wang revised the manuscript.

Funding

This work was supported by the National Natural Science Foundation of China (82373038, 81902923), the Natural Science Foundation of Henan (242300421480), Medical Technology Co-construction Project Fund of Henan (LHGJ20230256, LHGJ20230419), Medical Education Research Project of Henan Province (Wjlx2022214), Postdoctoral start-up fund of The First Affiliated Hospital of Zhengzhou University (71983).

Data availability

The data are available in the article and obtained from the corresponding author upon reasonable request.

Declarations

Ethical approval

All animal interventions were approved by approved by the Animal Ethics Committee of The First Affiliated Hospital of Zhengzhou University, China.

Consent for publication

All authors approved the manuscript for publication.

Conflict of interest

The authors declare that they have no competing interests.

Author details

¹Department of Oncology, the First Affiliated Hospital of Henan University, Kaifeng 475000, China

²Department of Medical Laboratory, Tongji Medical College, the Central Hospital of Wuhan, Huazhong University of Science and Technology, Wuhan 430030, China

³Department of Laboratory Medicine, Tongji Hospital, Tongji Medical College, Huazhong University of Science and Technology, Wuhan 430030, China

⁴Institute of Biology and Medicine, College of Life and Health Sciences, Wuhan University of Science and Technology, Wuhan 430081, China

⁵Gene Hospital of Henan Province, the First Affiliated Hospital of Zhengzhou University, Zhengzhou 450052, China

⁶Department of Gastrointestinal Surgery, the First Affiliated Hospital of Zhengzhou University, Zhengzhou 450052, China

⁷Translational Medicine Center, the First Affiliated Hospital of Zhengzhou University, Zhengzhou 450052, China

⁸College of Anesthesiology, Xinxiang Medical University, Xinxiang 453000, China

Received: 9 November 2024 / Accepted: 25 January 2025

Published online: 04 February 2025

References

- Bray F, Laversanne M, Sung H, Ferlay J, Siegel RL, Soerjomataram I, Jemal A. Global cancer statistics 2022: GLOBOCAN estimates of incidence and mortality worldwide for 36 cancers in 185 countries. *CA Cancer J Clin*. 2024;74:229–63.
- Aghapour SA, Torabizadeh M, Bahreiny SS, Saki N, Jalali Far MA, Yousefi-Avavand A, Dost Mohammad Ghasemi K, Aghaei M, Abolhasani MM, Sharifani MS, et al. Investigating the dynamic interplay between Cellular Immunity and Tumor cells in the Fight Against Cancer: an updated Comprehensive Review. *Iran J Blood Cancer*. 2024;16:84–101.
- Benedit P, Paciucci R, Thomson TM, Valeri M, Nadal M, Caceres C, de Torres I, Estivill X, Lozano JJ, Morote J, Reventos J. PTOV1, a novel protein overexpressed in prostate cancer containing a new class of protein homology blocks. *Oncogene*. 2001;20:1455–64.
- Guo F, Feng L, Hu JL, Wang ML, Luo P, Zhong XM, Deng AM. Increased PTOV1 expression is related to poor prognosis in epithelial ovarian cancer. *Tumour Biol*. 2015;36:453–8.
- Lei F, Zhang L, Li X, Lin X, Wu S, Li F, Liu J. Overexpression of prostate tumor overexpressed 1 correlates with tumor progression and predicts poor prognosis in breast cancer. *BMC Cancer*. 2014;14:457.
- Chen SP, Zhang LS, Fu BS, Zeng XC, Yi HM, Jiang N. Prostate tumor overexpressed 1 is a novel prognostic marker for hepatocellular carcinoma progression and overall patient survival. *Med (Baltim)*. 2015;94:e423.
- Hafner A, Bulyk ML, Jambhekar A, Lahav G. The multiple mechanisms that regulate p53 activity and cell fate. *Nat Rev Mol Cell Biol*. 2019;20:199–210.
- Vousden KH, Lane DP. p53 in health and disease. *Nat Rev Mol Cell Biol*. 2007;8:275–83.
- Liu Y, Su Z, Tavara O, Gu W. Understanding the complexity of p53 in a new era of tumor suppression. *Cancer Cell*. 2024;42:946–67.
- Liebl MC, Hofmann TG. The role of p53 signaling in Colorectal Cancer. *Cancers (Basel)* 2021, 13.
- Muller PA, Vousden KH. p53 mutations in cancer. *Nat Cell Biol*. 2013;15:2–8.
- Chen RH, Chen YH, Huang TY. Ubiquitin-mediated regulation of autophagy. *J Biomed Sci*. 2019;26:80.
- Xu Z, Wu W, Yan H, Hu Y, He Q, Luo P. Regulation of p53 stability as a therapeutic strategy for cancer. *Biochem Pharmacol*. 2021;185:114407.
- Shi Y, Norberg E, Vakifahmetoglu-Norberg H. Mutant p53 as a Regulator and Target of Autophagy. *Front Oncol*. 2020;10:607149.
- Wade M, Li YC, Wahl GM. MDM2, MDMX and p53 in oncogenesis and cancer therapy. *Nat Rev Cancer*. 2013;13:83–96.
- Dornan D, Wertz I, Shimizu H, Arnott D, Frantz GD, Dowd P, O'Rourke K, Koepfen H, Dixit VM. The ubiquitin ligase COP1 is a critical negative regulator of p53. *Nature*. 2004;429:86–92.
- Liu J, Zhang C, Xu D, Zhang T, Chang CY, Wang J, Liu J, Zhang L, Haffty BG, Zong WX et al. The ubiquitin ligase TRIM21 regulates mutant p53 accumulation and gain of function in cancer. *J Clin Invest* 2023, 133.
- Vousden KH, Prives C. Blinded by the light: the growing complexity of p53. *Cell*. 2009;137:413–31.
- Canovas V, Leonart M, Morote J, Paciucci R. The role of prostate tumor overexpressed 1 in cancer progression. *Oncotarget*. 2017;8:12451–71.
- Kimura S, Noda T, Yoshimori T. Dissection of the autophagosome maturation process by a novel reporter protein, tandem fluorescent-tagged LC3. *Autophagy*. 2007;3:452–60.
- Xie SA, Zhang W, Du F, Liu S, Ning TT, Zhang N, Zhang ST, Zhu ST. PTOV1 facilitates colorectal cancer cell proliferation through activating AKT1 signaling pathway. *Heliyon*. 2024;10:e36017.
- Cui Y, Ma W, Lei F, Li Q, Su Y, Lin X, Lin C, Zhang X, Ye L, Wu S, et al. Prostate tumour overexpressed-1 promotes tumorigenicity in human breast cancer via activation of Wnt/beta-catenin signalling. *J Pathol*. 2016;239:297–308.
- Liu J, Wu Y, Meng S, Xu P, Li S, Li Y, Hu X, Ouyang L, Wang G. Selective autophagy in cancer: mechanisms, therapeutic implications, and future perspectives. *Mol Cancer*. 2024;23:22.
- Liu F, Li Z, Wan S, Li Y, Ye Z, Li D. Pan-cancer analysis confirms the prognostic and immunological effects of prostate tumor overexpressed-1 in human cancers. *Curr Cancer Drug Targets* 2023.
- Wu Z, Liu Z, Jiang X, Mi Z, Meng M, Wang H, Zhao J, Zheng B, Yuan Z. Depleting PTOV1 sensitizes non-small cell lung cancer cells to chemotherapy through attenuating cancer stem cell traits. *J Exp Clin Cancer Res*. 2019;38:341.
- Alana L, Sese M, Canovas V, Punyal Y, Fernandez Y, Abasolo I, de Torres I, Ruiz C, Espinosa L, Bigas A, et al. Prostate tumor Overexpressed-1 (PTOV1) down-regulates HES1 and HEY1 notch targets genes and promotes prostate cancer progression. *Mol Cancer*. 2014;13:74.
- Marques N, Sese M, Canovas V, Valente F, Bermudo R, de Torres I, Fernandez Y, Abasolo I, Fernandez PL, Contreras H, et al. Regulation of protein translation and c-Jun expression by prostate tumor overexpressed 1. *Oncogene*. 2014;33:1124–34.
- Santamaria A, Castellanos E, Gomez V, Benedit P, Renau-Piqueras J, Morote J, Reventos J, Thomson TM, Paciucci R. PTOV1 enables the nuclear translocation and mitogenic activity of flotillin-1, a major protein of lipid rafts. *Mol Cell Biol*. 2005;25:1900–11.
- Leng RP, Lin Y, Ma W, Wu H, Lemmers B, Chung S, Parant JM, Lozano G, Hakem R, Benchimol S. Pirh2, a p53-induced ubiquitin-protein ligase, promotes p53 degradation. *Cell*. 2003;112:779–91.
- Murray-Zmijewski F, Slee EA, Lu X. A complex barcode underlies the heterogeneous response of p53 to stress. *Nat Rev Mol Cell Biol*. 2008;9:702–12.
- Rahman MA, Park MN, Rahman MH, Rashid MM, Islam R, Uddin MJ, Hannan MA, Kim B. p53 modulation of Autophagy Signaling in Cancer therapies: perspectives mechanism and therapeutic targets. *Front Cell Dev Biol*. 2022;10:761080.
- Vakifahmetoglu-Norberg H, Kim M, Xia HG, Iwanicki MP, Ofengied D, Coloff JL, Pan L, Ince TA, Kroemer G, Brugge JS, Yuan J. Chaperone-mediated autophagy degrades mutant p53. *Genes Dev*. 2013;27:1718–30.
- Luo P, Xu Z, Li G, Yan H, Zhu Y, Zhu H, Ma S, Yang B, He Q. HMGB1 represses the anti-cancer activity of sunitinib by governing TP53 autophagic degradation via its nucleus-to-cytoplasm transport. *Autophagy*. 2018;14:2155–70.
- Vargas JNS, Hamasaki M, Kawabata T, Youle RJ, Yoshimori T. The mechanisms and roles of selective autophagy in mammals. *Nat Rev Mol Cell Biol*. 2023;24:167–85.
- Zitkute V, Jasinevicius A, Vaitiekaitė G, Kukcinaviciute E, Aleksandraviciute B, Eidenaitė E, Sudeikis L, Jonusiene V, Sasnauskiene A. The role of p62 in cell death and survival of 5-fluorouracil and oxaliplatin-resistant colorectal cancer cells. *J Cell Biochem*. 2023;124:1779–91.
- Zhang J, Yang S, Xu B, Wang T, Zheng Y, Liu F, Ren F, Jiang J, Shi H, Zou B, et al. p62 functions as an oncogene in colorectal cancer through inhibiting apoptosis and promoting cell proliferation by interacting with the vitamin D receptor. *Cell Prolif*. 2019;52:e12585.
- Saki N, Haybar H, Aghaei M. Subject: motivation can be suppressed, but scientific ability cannot and should not be ignored. *J Transl Med*. 2023;21:520.
- Aghaei M, Khademi R, Bahreiny SS, Saki N. The need to establish and recognize the field of clinical laboratory science (CLS) as an essential field in advancing clinical goals. *Health Sci Rep*. 2024;7:e70008.

Publisher's note

Springer Nature remains neutral with regard to jurisdictional claims in published maps and institutional affiliations.